JOURNAL OF NEUROTRAUMA 29:776–788 (March 20, 2012)

DOI: 10.1089/neu.2010.1602

Mitochondrial Injury after Mechanical Stretch of Cortical Neurons *in vitro*: Biomarkers of Apoptosis and Selective Peroxidation of Anionic Phospholipids

Jing Ji,[1,2,*] Yulia Y. Tyurina,[1,2,*] Minke Tang,[3,4,*] Weihong Feng,[1,2] Donna B. Stolz,[5] Robert S.B. Clark,[3,4] David F. Meaney,[6] Patrick M. Kochanek,[3,4] Valerian E. Kagan,[1,2] and Hülya Bayır[1–4]

Abstract

Mechanical injury of neurites accompanied by rupture of mitochondrial membranes may lead to immediate nonspecific release and spreading of pro-apoptotic factors and activation of proteases, that is, execution of apoptotic program. In the current work, we studied the time course of the major biomarkers of apoptosis as they are induced by exposure of rat cortical neurons to mechanical stretch. By using transmission electron microscopy, we found that mitochondria in the neurites were damaged early (1 h) after mechanical stretch injury whereas somal mitochondria were significantly more resistant and demonstrated structural damage and degenerative mitochondrial changes at a later time point after stretch (12 h). We also report that the stretch injury caused immediate activation of reactive oxygen species production followed by selective oxidation of a mitochondria-specific phospholipid, cardiolipin, whose individual peroxidized molecular species have been identified and quantified by electrospray ionization mass spectrometry analysis. Most abundant neuronal phospholipids – phosphatidylcholine, phophatidylethanolamine – did not undergo oxidative modification. Simultaneously, a small-scale release of cytochrome c was observed. Notably, caspase activation and phosphatidylserine externalization – two irreversible apoptotic events designating a point of no return – are substantially delayed and do not occur until 6–12 h after the initial impact. The early onset of reactive oxygen species production and cytochrome c release may be relevant to direct stretch-induced damage to mitochondria. The delayed emergence of apoptotic neuronal death after the immediate mechanical damage to mitochondria suggests a possible window of opportunity for targeted therapies.

Key words: cardiolipin; *in vitro* traumatic brain injury; mitochondria; oxidative lipidomics; oxidative stress

Introduction

Several interrelated pathways of cell death – necrosis, autophagy and apoptosis – can occur after traumatic brain injury (TBI) (Brophy et al., 2009; Clark et al., 2008; Liu et al., 2008; Pedersen et al., 2009). The major biological role of apoptosis is to eliminate cells with irreparably damaged DNA to prevent spillover and penetration of the genotoxic contents into surrounding proliferating cells (Fadeel, 2003). Cell death program includes a series of mitochondrial events culminating in activation of protease (caspase) cascades – a point of no return in apoptosis (Polster and Fiskum, 2004; Samali et al., 1999; Zhivotovsky et al., 1999). Among early mitochondrial events are the production of reactive oxygen species (ROS), translocation of pro-apoptotic Bcl-2-family proteins Bax and Bak, permeabilization of mitochondrial membrane, and release of pro-apoptotic factors into the cytosol (Cardaci et al., 2008; Kroemer et al., 2007; Lahiry et al., 2008; Li et al., 1999; Polster and Fiskum, 2004). This highly coordinated chain of events provides for complete and effective disassembly of intracellular contents – the goal of apoptosis (Fadeel, 2003; Kroemer et al., 2007).

Neurons contain two different pools of mitochondria – one in synaptic terminals, and the other in the central soma (Lai et al., 1977). Although genotoxic effects and their consequences may represent only a limited risk for post-mitotic

[1]Center for Free Radical and Antioxidant Health, [2]Department of Environmental and Occupational Health, [3]Safar Center for Resuscitation Research, [4]Department of Critical Care Medicine, [5]Department of Cell Biology and Physiology, University of Pittsburgh, Pittsburgh, Pennsylvania.
[6]Department of Bioengineering, University of Pennsylvania, Philadelphia, Pennsylvania.
*These authors contributed equally to this work.

neurons, damage to their mitochondria may trigger pro-apoptotic events. In particular, mechanical injury of neurites resulting in rupture of mitochondrial membranes may be associated with elevated risk of apoptosis caused by non-specific release of pro-apoptotic factors and activation of proteases (Arundine et al., 2004; Bayir et al., 2007; Fiskum, 2000; Slemmer et al., 2008).

Establishing and understanding the mechanisms underlying TBI-induced neuronal death may be important for developing new therapeutic strategies based on the prevention of the spreading of apoptotic signaling by blocking the upstream events. One of them is recently discovered interactions of a mitochondria-specific phospholipid, cardiolipin (CL), with an inter-membrane space protein, cytochrome c (cyt c) (Iverson and Orrenius, 2004; Kagan et al., 2005; Petrosillo et al., 2006). These two molecules form a complex with peroxidase activity that catalyzes CL peroxidation, and facilitates mitochondrial permeability transition and release of pro-apoptotic factors, including cyt c, into the cytosol (Kagan et al., 2005). Prevention of cyt c release may be achieved by suppression of CL oxidation (Borisenko et al., 2008; Jiang et al., 2008; Kagan et al., 2009). Experimentally, this may be tested using an *in vitro* impact model of mechanical stretch to neurons where the rupture of mitochondria is not complicated by other cell–cell interactions affecting the pro-apoptotic events.

Here, we studied the time course of the major biomarkers of apoptosis induced by mechanical stretch in cortical neurons. We hypothesized that mechanical stretch injury of neurons is associated with immediate damage to mitochondria in neurites and subsequent triggering of apoptosis accompanied by CL oxidation. We report that the stretch causes immediate damage to neurons that includes CL oxidation and cyt c release. The secondary damage is separated from the former by several hours and is evidenced by caspase activation and phosphatidylserine (PS) externalization. The delayed emergence of apoptotic neuronal death suggests a possible window of opportunity for targeted therapies.

Methods

Reagents

All chemicals were purchased from Sigma Chemicals (St. Louis, MO) unless otherwise noted.

Isolation and culture of cortical neurons

Animal procedures were performed in accordance with the University of Pittsburgh Animal Care and Use Committee. Primary cortical neuronal cultures were prepared from embryonic day 17 rats. Pregnant Sprague–Dawley rats (Harlan Laboratories, Indianapolis, IN) were anesthetized with CO_2 and killed via decapitation. Embryos were surgically removed from the adult rat and cortices were isolated separately in ice-cold Neurobasal medium (Invitrogen, Carlsbad, CA) supplemented with B-27 (Invitrogen, Carlsbad, CA) and penicillin-streptomycin (Invitrogen, Carlsbad, CA). Tissue was then rinsed twice with the same medium and set in 0.25% trypsin with EDTA (Invitrogen, Carlsbad, CA) for 15 min at 37°C. The tissue was again rinsed twice and triturated in ice-cold Neurobasal medium to obtain neuronal cell suspension.

Cells were plated at 2.0×10^6 cells per ml (3.5 mL/well) onto thin, clear, flexible silicone membranes (Specialty Manufacturing, Saginaw, MI) treated with 0.05% poly-D-lysine hydrobromide (Sigma-Aldrich, St. Louis, MO) for 2 h at room temperature (RT), rinsed twice with Hanks' Balanced Salt Solution (Invitrogen, Carlsbad, CA), and allowed to dry under a laminar flow hood for 1 h. Experiments were performed at 7–9 days, when cultures consist primarily of neurons (> 95% microtubule-associated protein [MAP2] immunopositive cells, < 5% glial fibrillary acidic protein immunopositive cells). The culture medium was changed every 2 days.

In vitro *TBI model*

Trauma was produced using a well established *in vitro* model (Lusardi et al., 2004). Briefly, primary neuronal cells cultured on silicone membranes were subjected to a computer- controlled quantifiable mechanical insult by displacing the membrane over a hollowed platform. The membranes were stretched with a known pre-tension across the surface of custom-designed, stainless steel wells that fit into the cell stretch apparatus. Cultures were subjected to a severe mechanical stretch, consisting of a rapid onset strain pulse ($10\,s^{-1}$ strain rate and 50% membrane deformation). Severe stretch was chosen in order to simulate a strain field similar to what occurs in animal models of severe TBI. Sterile technique was strictly followed in all procedures. The neuronal cultures were either returned to the incubator for further observation or subjected to further treatment dependent upon the experiment after mechanical stretch.

Assessment of neuronal viability

Cell viability was assessed using the Alamar blue (Invitrogen, Carlsbad, CA) assay, 3-[4,5-dimethylthiazol-2-yl-]-2,5-diphenyltetrazolium bromide (MTT) assay, and trypan blue dye exclusion assay. Alamar blue assay is based on conversion of cell permeable non-fluorescent compound resazurin to a fluorescent molecule, resorufin, by the reducing environment of living cells (Gartlon et al., 2006; Gil-ad et al., 2001; Shimazawa and Hara, 2006; Shimazawa et al., 2007; Yang et al., 2000). Cell viability was assessed by the use of 10% resazurin solution for 3 h at 37°C, and then cells were examined for fluorescence at 560/590 nm. Fluorescence was expressed as a percentage of that in control cells (after subtraction of background fluorescence). The MTT solution (5 mg MTT/mL medium) was added to each well 24 h after mechanical stretch at the final concentration of 250 μM and incubated for 3 h. The medium was removed, and cells were dissolved in dimethyl sulfoxide (DMSO). Optical density was determined using a spectrophotometer (Spectra MAX 340, Molecular Devices, Sunnyvale, CA) at 550-nm test and 690-nm reference wavelengths. Neurons were stained with trypan blue, and viability was determined using the trypan blue exclusion assay. Neurons were incubated with 0.4% trypan blue in HBSS for 2 min at room temperature. Neurons were observed under the microscope and counted as stained and unstained cells on a hemacytometer separately, then viable cell ratios were calculated according to the following formula: viable cell ratio (%) = (unstained cell number/total cell number)*100%.

Transmission electron microscopy (TEM)

Neurons were fixed with 2.5% glutaraldehyde in phosphate buffered saline (PBS) (pH = 7.4) for 2 h at RT, then

washed, and monolayers of neurons were postfixed in 1% OsO_4 and 1% $K_3Fe(CN)_6$ for 1 h at 4°C. After three washings with PBS, the monolayers were dehydrated through a graded series of 30% to 100% ethanol, and then incubated in Polybed 812 epoxy resin (Polysciences, Warrington, PA) for 1h. After several changes of 100% resin (three times for 1 h each), monolayers were polymerized at 37°C overnight with additional hardening at 60°C for 48 h. Ultrathin (60 nm) sections were collected on 200 mesh grids and stained with 2% uranyl acetate in 50% methanol for 10 min followed by 1% lead citrate for 7 min. Sections were observed on a JEM 1210 electron microscope (JEOL, Peabody, MA) at 80 kV.

Assessment of mitochondrial superoxide production with MitoSOX

The mitochondrial superoxide production was measured by flow cytometry as described ([Ainslie et al., 2008] and http://bts.ucsf.edu/desai/protocols.html). Briefly, MitoSOX Red (Invitrogen, Carlsbad, CA) was added to the neuronal cultures at a final concentration of 3 μM. The cells were incubated at 37 °C for 5 min to allow loading of MitoSOX Red. The neuronal cultures were then fixed with same volume of 4% paraformaldehyde (in PBS, pH7.4) and incubated at RT for 30 min. The cells were then detached with 0.1% trypsin and then spun down 600*g* at 4 °C for 3 min. The cells were washed two times with PBS and placed in a sterile FACS tube at a concentration of $5 \sim 10 \times 10^6$ cells per 100 μL. Cells were stored at 4°C for a maximum of 30 min until the samples were analyzed via flow cytometer (Becton-Dickinson, Franklin Lakes, NJ). Hoechst 33258 (1 μg/mL; Molecular Probes) was added 1 min before flow cytometer analysis.

Mitochondrial cyt c release

Neuronal cells (1×10^7) were washed in PBS then incubated for 3 min in lysis buffer (75 mM NaCl, 8 mM Na_2HPO_4, 1 mM NaH_2PO_4, 1 mM EDTA, and 350 μg/mL digitonin). The lysates were centrifuged at 12,000*g* for 1 min, and the supernatant was collected for cytosolic cyt c analysis. The mitochondria-enriched fraction was resuspended in lysis buffer (25 mM HEPES-KOH pH 7.6; 5 mM $MgCl_2$, 0.5 mM EDTA, 10% glycerol, 1 mM dithiothreitol [DTT], 1 mM phenylmethylsulfonyl fluoride [PMSF]). The suspension was then incubated on ice and sonicated twice for 10 sec each time with a 30-sec interval. The final mitochondrial lysate was spun at 400,000*g* in an ultracentrifuge (Backman, Fullerton, CA) at 4°C for 25 min. The supernatant was collected for mitochondrial cyt c analysis. Cyt c was detected with Western blot analysis.

Caspase activity

Caspase 3/7 activity was measured using a luminescence Caspase-Glo assay kit obtained from Promega (Madison, WI). Luminescence was determined at baseline and after 1 h incubation at RT using a Fusion-α plate reader (Perkline Cop., Boston MA). Caspase 3/7 activity was expressed as the luminescence produced after 1 h incubation per mg of protein.

PS externalization

Externalization of PS was analyzed by flow cytometry using an Annexin V kit (Biovision, Mountain View, CA). Briefly, cells were harvested at the end of incubation, and then stained with Annexin V-FITC and propidium iodide (PI) prior to analysis. Ten thousand events were collected on a FACScan flow cytometer equipped with a 488-nm argon ion laser and supplied with the Cell Quest software. Cells that were Annexin V-positive and PI-negative were considered as apoptotic cells.

Cytotoxicity detection (lactate dehydrogenase [LDH] release)

The effect of pretreatment with *N*-acetylcysteine and z-VAD-FMK on cortical neuronal cell injury was quantified by the measurement of LDH at 24 h after the insult. An aliquot of bathing media was combined with NADH and pyruvate solutions. LDH activity is proportional to the rate of pyruvate loss, which was assayed by absorbance change by using a microplate reader (Spectra MAX 340, Molecular Devices, Sunnyvale, CA). Blank LDH levels were subtracted from insult LDH values and results normalized to 100% neuronal death caused by 0.5% Triton X-100 exposure.

Western blot analyses

Cell samples were separated by standard sodium dodecyl sulfate-polyacrylamide gel electrophoresis (SDS-PAGE) and transferred to polyvinylidene difluoride membrane by tank blotting method. Nonspecific binding sites were blocked using 5% nonfat milk containing 0.1% Tween-20 in PBS (pH 7.4). Thereafter, membranes were probed overnight at 4°C with mouse monoclonal anti-4-hydroxynonenal antibody (HNE, 1 μg/mL, clone 198960, R&D systems, Minneapolis, MN), or mouse monoclonal anti-cyt c antibody (1:400, clone 7H8.2C12, MAB1800, Millipore, Billerica, MA) diluted in 5% nonfat milk containing 0.1% Tween-20 in PBS (pH 7.4). After three washes with 0.1% Tween-20 in PBS (pH 7.4), immune complexes were labeled for 2 h with horseradish peroxidase-conjugated anti-mouse IgG (1:2000, Cell Signaling Technology, Inc. Danvers, MA). After five washes, bound antibodies were visualized by ECL Western Blotting Substrate Kit (Mountain View, CA).

Immunocytochemistry

Neurons were fixed in 2% paraformaldehyde and then incubated with 5% normal donkey serum and 2% bovine serum albumin in PBS containing 0.2% Triton X-100 for 1 h and then incubated overnight at 4°C with primary antibody against MAP2 (1:500, Abcam, Cambridge, MA), followed by an incubation with donkey anti-mouse IgG Alexa Fluor 488 conjugated secondary antibody (1:1000, Invitrogen, Carlsbad, CA) for 1 h at RT. Sections were washed four times in PBS at RT in the dark, with the last wash containing 10 μg/mL 4′,6-diamidino-2-phenylindole (DAPI). Cells were examined under inverted florescent microscope Leica DM-IL (Leica, Wetzlar, Germany) equipped with a digital Leica DC300 camera (Leica, Wetzlar, Germany).

Lipid analysis

Total lipids were extracted from neurons by the Folch procedure (Folch et al., 1957). Lipids were separated by two-dimensional high performance thin layer chromatography (2D-HPTLC) (Rouser et al., 1970). To prevent oxidative modification of phospholipids during separation, plates were

treated with methanol containing 1 mM EDTA, 100 μM diethylene triamine pentaacetic acid (DTPA) prior to separation of phospholipids by 2D-HPTLC. The phospholipids were visualized by exposure to iodine vapors and identified by comparison with authentic phospholipid standards. Lipid phosphorus was determined by a micro-method (Böttcher et al., 1961).

Electrospray ionization mass spectrometry (ESI-MS) analysis of phospholipids

ESI-MS analysis was performed by direct infusion into a linear ion-trap mass spectrometer LXQ^{TM} with the Xcalibur operating system (Thermo Fisher Scientific, San Jose, CA). Samples collected after 2D-HPTLC separation were evaporated under N_2, re-suspended in chloroform:methanol 1:1 v/v (20 pmol/μL) and directly utilized for acquisition of negative-ion or positive-ion ESI mass spectra at a flow rate of 5 μL/min. The ESI probe was operated at a voltage differential of 3.5–5.0 kV in the negative or positive ion mode. Capillary temperature was maintained at 70 or 150°C. MSn analysis was performed using isolation width of 1 m/z, five microscans with maximum injection time 1000 ms. Full-scan ESI-MS analysis in the negative ionization mode was used for all phospholipids classes. Additionally, MS-spectra were recorded in positive mode for phosphatidylcholine (PC) and sphingomyelin (Sph). Two ion activation techniques were used for MS analysis: collision-induced dissociation (Q = 0.25, low mass cutoff at 28% of the precursor m/z) and pulsed-Q dissociation technique, with Q = 0.7, and no low mass cutoff for analysis of low molecular weight fragment ions (Schwartz et al., 2005). Based on MS fragmentation data, chemical structures of lipid molecular species were obtained using ChemDraw and confirmed by comparing with the fragmentation patterns presented in Lipid Map Data Base (www.lipidmaps.org).

Quantification of oxidized molecular species of phospholipids

Lipid hydroperoxides were determined by fluorescence high performance liquid chromatography (HPLC) of resorufin formed in peroxidase-catalyzed reduction of specific phospholipid hydroperoxides with Amplex® Red (*N*-acetyl-3, 7-dihydroxyphenoxazine, Molecular Probes, Eugene, OR) as previously described (Tyurin et al., 2008). In addition, liquid chromatography (LC)/ESI-MS was used for quantitative analysis of oxidized phospholipids as well. LC/MS of phospholipids was performed with Dionex Ultimate^{TM} 3000 HPLC coupled online to a linear ion trap mass spectrometer (LXQ Thermo-Fisher, San Jose, CA). The lipids were separated on a normal phase column (Luna 3 μm Silica 100A, 150 × 2 mm [Phenomenex]) with flow rate 0.2 mL/min using gradient solvents containing 5 mM CH_3COONH_4 (A - hexane:propanol:water, 43:57:1 [v/v/v] and B - hexane:propanol:water, 43:57:10 [v/v/v]).

Statistical analysis

The results are presented as mean ± SD unless otherwise specified, with values from at least three independent experiments, and statistical analyses were performed by either

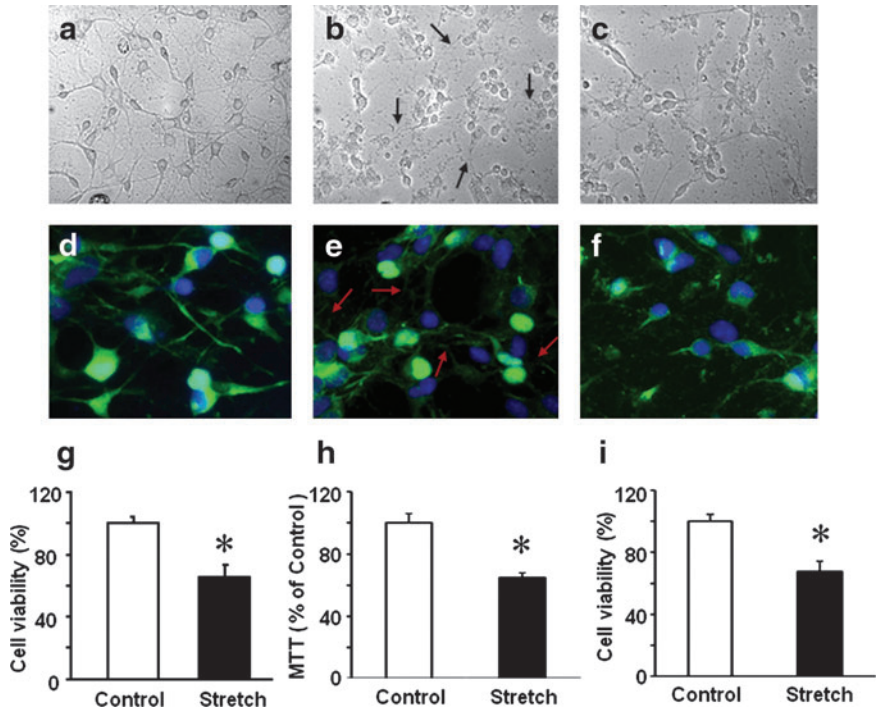

FIG. 1. Viability of cortical neurons after stretch injury. Representative photomicrographs of control cortical neurons (**a, d**) and cortical neurons after mechanical stretch, 10 s^{-1} strain rate and 50% membrane deformation (**b**, **c, e, f**). Stretch injury resulted in damage to the neuronal processes whereas the cell bodies remained intact and attached to the substrate, immediately after stretch (*arrows*, **b, e**), and at 24 h after stretch (**c, f**). Green: microtubule associated protein 2 (MAP2) immunostain; Blue: DAPI stain. Quantification of cell viability at 24 h after stretch injury using Alamar Blue (**g**) and MTT (**h**) assays and trypan blue (**i**) staining. Data are mean ± SD, *$p < 0.05$ vs control, $n = 6$. Color image is available online at www.liebertonline.com/neu

unpaired Student t test or one-way ANOVA. The statistical significance of differences was set at $p < 0.05$.

Results

Morphological analysis of neuronal cells

Microscopic examination revealed that the characteristic morphology of control neurons (Fig. 1a, d) with neurites was disrupted by mechanical stretch: an immediate damage to the neurites was evident while the cell bodies remained intact and attached to silastic membranes (Fig. 1b, e). There was no obvious recovery of cells at 24 h after injury (Fig. 1c, f). Assessments of cell viability demonstrated that ~35% of neuronal cells were dead 24 h after stretch (Fig. 1g–i).

TEM evaluation of neurons showed differences in the mitochondrial morphology between sham and stretched neurons (Fig. 2). Mitochondria in both soma and neurites in control neurons appeared normal with clear cristae structure (Fig. 2a). Early after injury (1 h), the mitochondria in the neurites were swollen and their cristae were distorted, whereas the mitochondria in the soma of neurons appeared similar to those in control neurons (Fig. 2b). However, at later time points (12–24 h) after the injury, abnormal mitochondria were observed in both the soma and neurites (Fig. 2c, f, and g). Furthermore, dying neurons showed features of apoptosis with intact plasma membrane, fragmented nuclei, chromatin clumping, and cytoplasmic vacuoles as well as necrosis with loss of membrane integrity and cell swelling (Fig. 2 e–g).

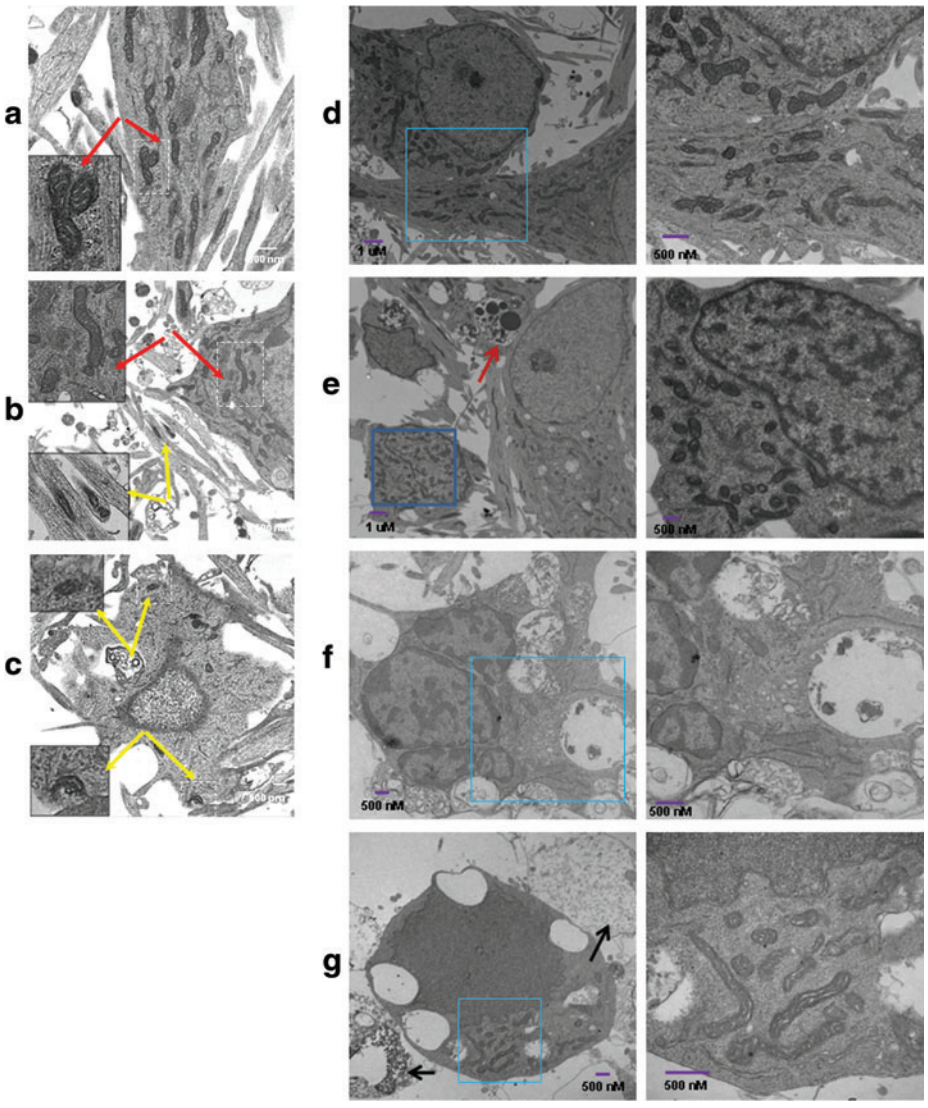

FIG. 2. Ultrastructural changes induced by mechanical stretch through transmission electron microscopy (TEM). Typical TEM image of control neurons (**a**) and cortical neurons 1h (**b**) and 12 h (**c**) after mechanical stretch. Representative TEM images are presented. Red (**a, b**) and yellow (**b, c**) arrows indicate normal and damaged mitochondria, respectively. (**d**) A representative section of control primary cortical neurons with dispersed chromatin and a clearly defined nucleolus. (**e–g**) A representative section of mechanically stretched primary cortical neurons showing apoptosis with intact plasma membrane, fragmented nuclei, chromatin clumping, and cytoplasmic vacuoles in 6 h (**e**), 12 h (**f**) and 24 h (**g**). Enlargement of the rectangular selected areas show the normal (**d**) or abnormal (**f, g**) mitochondria after mechanical stretch. Red arrow (**e**) indicates apoptotic bodies. Black arrows (**g**) indicate necrotic neurons with loss of membrane integrity and cell swelling. Color image is available online at www.liebertonline.com/neu

Mitochondrial ROS production, biomarkers of mitochondrial damage and apoptosis

Analysis of mitochondrial ROS production by MitoSOX using flow cytometry (Fig. 3) revealed a two-phase response to stretch. The initial very rapid production of ROS detectable at early time points (0.5 and 1 h) was followed by a slower, yet significant incremental growth at later time points (up to 24 h).

One can assume that stretch-induced rapid damage of mitochondria in neurites might be associated with the release of their cyt c. Indeed, there was a substantial (>2.5-fold) release of cyt c from mitochondria into the cytosol already observed at 0.5 h after the exposure (Fig. 4a). Cyt c release displayed a two-phase response whereby the initial early release reached a plateau at 1 h. Maximal release of cyt c was observed at 6 h and reached a plateau thereafter. Notably, significant amounts of cyt c remained confined within the mitochondrial compartments during both the earlier and later time points after the impact. Two important biomarkers usually associated with post-mitochondrial stages of apoptosis – caspase activation and PS externalization – revealed significant increases after stretch injury. Caspase −3/7 activity was significantly increased only at time points as late as 12 and 24 h (Fig. 4b). A slight increase in Annexin V positivity was detected as early as 0.5 h after stretch (Fig.4c). At 12 and 24 h after stretch injury, a large increase in the number of Annexin V-positive cells associated with PS externalization was observed (Fig. 4c). PI positivity – corresponding to necrosis – followed the same trend with a lower magnitude. Pre-treatment with z-VAD-FMK improved cell survival as assessed by Annexin V/PI and LDH assays (Fig. 4 d, e).

In order to dissect the primary mechanical stretch-induced injury versus secondary oxidative stress-induced damage to neurites, we pre-treated neurons with an antioxidant, *N*-acetylcysteine. This resulted in a significant decrease in cell death as assessed by PI and Annexin V positivity as well as by LDH viability assay (Fig. 4 d, e). This suggests that both the primary injury to neurites and the secondary oxidative stress-dependent damage contributed to neuronal death after stretch.

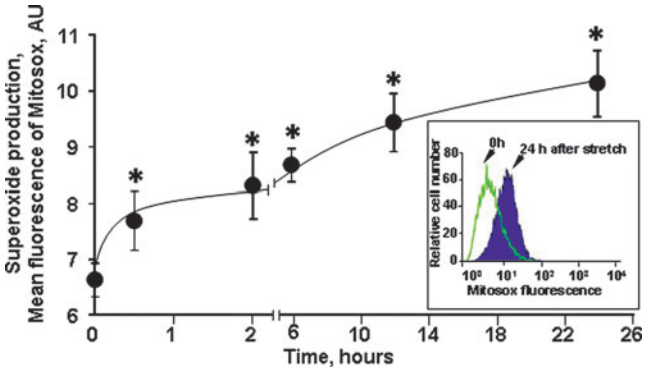

FIG. 3. Time course of mitochondrial superoxide generation in cortical neurons after stretch injury assessed by flow cytometry. Insert: histograms demonstrating MitoSOX flouorescence intensities in control neurons and neurons 24 h after stretch. Data are mean ± SEM, $^*p < 0.005$ vs. control, $n = 6$. Color image is available online at www.liebertonline.com/neu

Oxidation of phospholipids in stretched neurons

No significant changes in the phospholipid composition in stretched neurons were found (Fig. 5a). Moreover, all major classes of phospholipids – PC, phosphatidylethanolamine (PE), phosphatidylinositol (PTI), PS, and CL – contained polyunsaturated fatty acid residues with 2, 3, 4, 5, and 6 double bonds, the major peroxidation substrates. Notably, a robust oxidation of CL – a mitochondria-specific phospholipid – was clearly detectable 2 h after the stretch exposure. A smaller scale oxidation of PS was also observed in stretched neurons 2 h after injury (Fig. 5b; Fig. 6c). No significant oxidation was detectable in most dominant phospholipid classes – PC, PE and PTI.

To more specifically characterize oxidation of CL and PS, LC-ESI-MS analyses were performed. Typical LC-ESI-MS spectra of CL and PS isolated from primary neurons are presented in Figure 6a and b, respectively. We found that CL molecular species containing linoleic, arachidonic, and docosahexaenoic acids were oxygenated. Moreover, several types of CL oxidation products – with one, two, three, and four oxygens were accumulated in stretched neurons (Fig. 6c). Among PS molecular species, the ones with oxygenated docosahexaenoic acid were predominantly found in stretched neurons. However, quantitatively, CL underwent a 7.5-fold more robust oxidation than PS. Overall, the results on stretch-induced peroxidation of phospholipids are summarized as a "Hit-map" (Fig. 6d).

Interestingly, evaluation of a nonspecific product of lipid peroxidation, namely 4-HNE adducts with proteins, revealed an early increase (Fig. 7). The 20 kDa band increased at 2 h and remained high at 12 and 24 h compared to respective control. The increase in 50 kDa band was more delayed and occurred at 12 h and remained high at 24 h compared to control.

Discussion

Derangements in mitochondrial functions have been observed in *in vivo* models and humans after TBI (Okonkwo and Povlishock, 1999; Robertson, 2004; Singh et al., 2006; Sullivan et al., 1999; Verweij et al., 1997; Xiong et al., 1997). The central role of mitochondria in intrinsic apoptotic pathways makes cells vulnerable to initiation and progression of death program upon the rupture of the organelles and release of pro-apoptotic factors. Brain trauma and mechanical stretch injury of neurons may be associated with the breakage of their neurites. It is possible that this will be associated with the mitochondrial mechanical injury and triggering of apoptosis. This implies that suppression of mitochondrial events leading to the release of pro-apoptotic factors may limit trauma-associated death of neurons.

Based on intracellular localization, two populations of neuronal mitochondria have been described that include non-synaptic (somal) and synaptic mitochondria (Lai et al., 1977). These two types of mitochondria display different metabolic activities, possibly associated with specific features of the phospholipid composition of their membranes (Kiebish et al., 2008). In particular, levels of CL were found to be lower, whereas levels of ceramide and PS were higher in synaptic than in somal mitochondria (Kiebish et al., 2008). Because CL molecules contain four fatty acid residues, they may include many different individual molecular species that can be distinguished by MS-analysis (Sparvero et al., 2010). Notably, molecular speciation of CLs in somal and synaptic

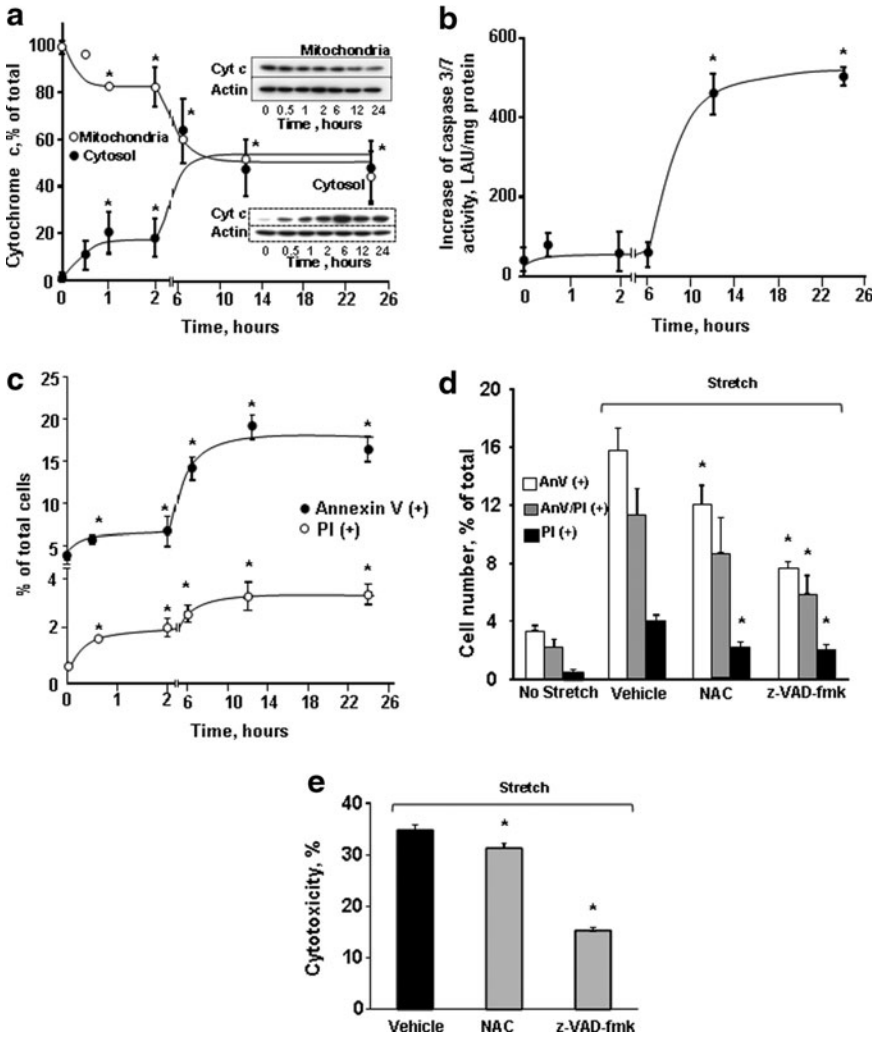

FIG. 4. Mechanical stretch-induced apoptosis in cortical neurons. (**a**) Release of cyt c after stretch injury in cortical neurons. Typical Western blots (insets) and the densitometric analysis of cyt c in mitochondrial (closed circles) and cytosolic (open circles) fractions of neuronal cells. Data are mean ± SD, $*p < 0.05$ vs control, $n = 3$. Note that release of cyt c from mitochondria occurred as early as 30 min after the the insult and peaked at 6 hrs after stretch injury. (**b**) Changes of caspase 3/7 activity in cortical neurons after stretch injury. Caspase 3/7 activity increased significantly at 12 h after stretch. The activity remained high at 24 h after injury. Data are mean ± SD, $*p < 0.05$ vs control, $n = 6$. (**c**) Flow cytometry analysis of Annexin V and propidium iodide (PI) responses of cortical neurons to stretch. Early Annexin V-positivity (phosphatidylserine [PS] externalization) - indicating apoptosis – was markedly enhanced 6 h after stretch. PI positivity – corresponding to necrosis – followed the same trend with a lower magnitude. Data are mean ± SD, $*p < 0.05$ vs control, $n = 3$. Effect of pre-treatment with antioxidant *N*-acetyl cysteine (NAC, 250 μM) and caspase inhibitor (z-VAD-fmk, 25 μM) on stretch-induced neuronal death assessed by flow cytometry analysis of PS externalization and PI positivity (**d**) and cytotoxicity (lactate dehydrogenase [LDH] release) relative to Triton exposure (**e**) at 24 h after stretch. Data are mean ± SD, $*p < 0.05$ vs respective vehicle group, $n = 4$.

mitochondria was found to be similar (Kiebish et al., 2008). The total amount and the diversity of CLs are dependent upon the *de novo* synthesis and remodeling, respectively (Schlame, 2008). Therefore, it is likely that remodeling of CLs is similar, whereas its synthesis is different in synaptic and somal mitochondria of neurons. We found that mitochondria in the neurites were damaged at early time points after mechanical stretch injury, whereas somal mitochondria were significantly more resistant and demonstrated features of structural damage much later after the stretch.

One of the possible reasons for the preferential damage to neurite mitochondria versus soma could be in the mechanical strain imposed on neurites versus soma. It is difficult to know the exact strain distribution for neurites and soma that we examined in our model; however, data from other mechanical cell injury models suggest that the magnitude and orientation of principal strains vary spatially and temporally and depend upon cell morphology. It was shown (Barbee et al., 1994; Kilinc et al., 2008) that fluid shear stress injury on cultured primary chick forebrain neurons caused axonal beading and localized cytoskeletal damage. Beads contained accumulated mitochondria and co-localized with focal microtubule disruptions. Laplaca and Thibault used a device that is a parallel disk viscometer applying fluid shear stress with variable rate

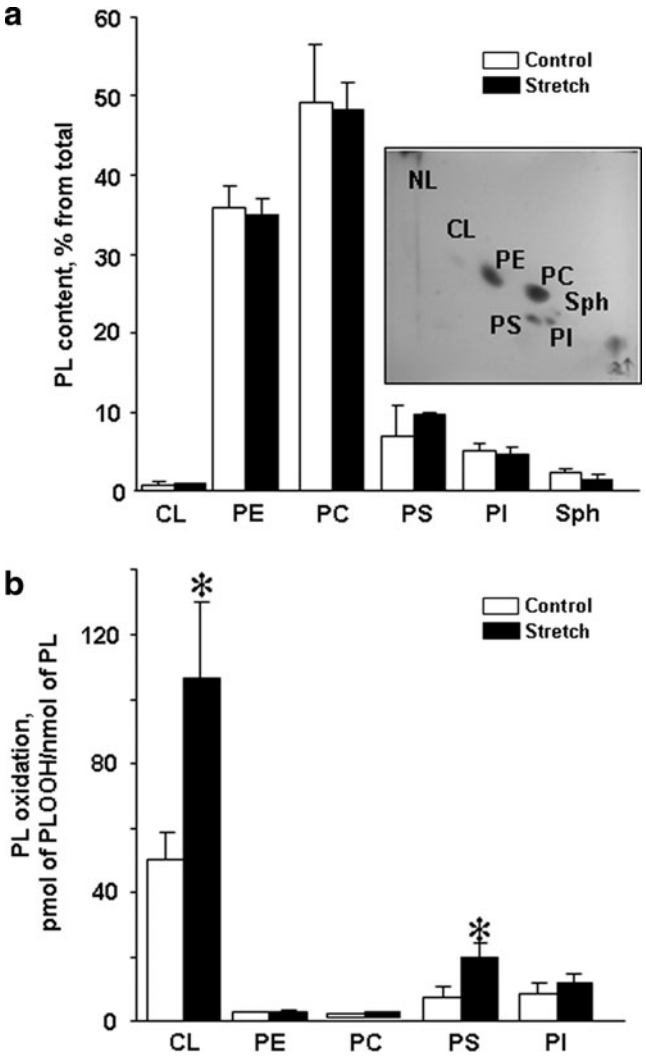

FIG. 5. Phospholipid composition and accumulation of phospholipid hydroperoxides in rat cortical neurons after stretch. (**a**) Phospholipid composition of control and stretched neurons. Insert: Typical two-dimensional high performance thin layer chromatography (2D-HPTLC) of lipids extracted from rat cortical neurons. Total lipids were extracted and separated by 2D-HPTLC. (**b**) Content of phospholipid hydroperoxides in control and stretched neurons. Two hours after stretch, total lipids were extracted, separated by 2D-HPTLC and phospholipid hydroperoxides (PL-OOH) were determined using Amplex® Red protocol. $*p < 0.05$ stretched vs. control neurons. PL, phospholipids; CL, cardiolipin; PE, phosphatidylethanolamine; PC, phosphatidylcholine; PS, phosphatidylserine; PI, phosphatidylinositol; Sph, Sphingomyelin.

of onset (LaPlaca and Thibault, 1997). They showed that the strain and strain rate for cell bodies and processes of the NT2-N cells (teratoma-derived human neuron like cells) varied widely for a given shear stress stimulus and arrangement. Cells in clumps of four or more had lower average strains than did single neurons or neurites. The wide range of strains observed could be caused by the variation in local forces, the organization and morphology of the neurons, and the spatial orientation and location of the cells and processes on the cell plate. In culture, cell bodies contain fewer adhesion sites as compared to cell processes, and therefore may be less susceptible to mechanical damage in our model. At the tissue level, however, other cell types and the microvascular environment support forces differently from neurons, and have different biochemical responses to traumatic stimuli (Murphy and Horrocks, 1993; LaPlaca et al., 1997). It is also worth mentioning that in neurons, mitochondria are organized in a network – mitochondrion – connected to other membrane structures and systems such as endoplasmic reticulum, nucleus and the cytoskeleton (Kuznetsov et al., 2009, Mironov, 2009). Therefore, any strain will be acting not on isolated mitochondria but on the entire branched system; it is possible that structural specificity of mitochondrion in neurites is different from that in the somal area – therefore contributing to the different response to mechanical strain.

Mitochondrial superoxide production has been implicated in trauma-induced neuronal death (Lewen et al., 2001; Sullivan et al., 1999). Mitochondria targeted hydroethidine (mito-hydroethidine or MitoSOX) became a very popular fluorogenic probe for detecting mitochondrial superoxide radical anion; however, its specificity has been recently questioned (Zielonka and Kalyanaraman, 2010). While the reaction between superoxide and mito-hydroethidine generates a specific red fluorescent product, mito-2-hydroxyethidium, another red fluorescent product, mito-ethidium, is also formed, usually at a much higher concentration than 2-hydroxyethidium. Both oxidation products of mito-hydroethidine bind to mitochondrial DNA with a concomitant manyfold ($\sim$40-fold) increase in the quantum yield of fluorescence. Therefore, it is likely that DNA-bound mito-hydroethidine oxidation product(s) will be the major contributors to the detectable fluorescence response. We used flow cytometry for quantitative analysis of MitoSOX data (Fig. 3). According to our protocol, MitoSOX was added to the neuronal cultures and incubated for 5 min after which the cells were fixed with 4% paraformaldehyde to stop the reaction. A similar protocol for flow cytometry using 3.7 % paraformaldehyde after incubation of cells with MitoSOX has been followed in previous studies (Ainslie et al., 2008). We believe that mitochondrial DNA-bound mito-hydroethidine oxidation products are not readily diffusible from paraformaldehyde-treated cells. Further, we did not correct the MitoSOX distribution across plasma and mitochondrial membrane because of a possible stretch-induced decrease of membrane potentials. Elegant studies by Johnson-Caldwell and associates have shown that a partial depolarization of either membrane could lead to an underestimation of superoxide levels. Clearly, such a correction would have enhanced the difference between the control and stretched samples. We can also add to this that the activity of intracellular esterases catalyzing the hydolysis of triphenylphosphonium moiety, which targets MitoSOX into mitochondria, might be another factor potentially affecting the fluorescence readouts. Overall, however, a relatively poor specificity of mito-hydroethidine for superoxide anion, rather than other possible deficiencies of the technique (such as effects of paraformaldehyde, dependence upon the mitochondrial membrane potential), may be a matter of major concern. Therefore, in the current study, we used other independent measures of oxidative stress – Western blotting of HNE-protein adducts and oxidative lipidomics analysis.

Compared to previous studies evaluating intrinsic caspase-mediated apoptosis in primary cortical neurons, the time

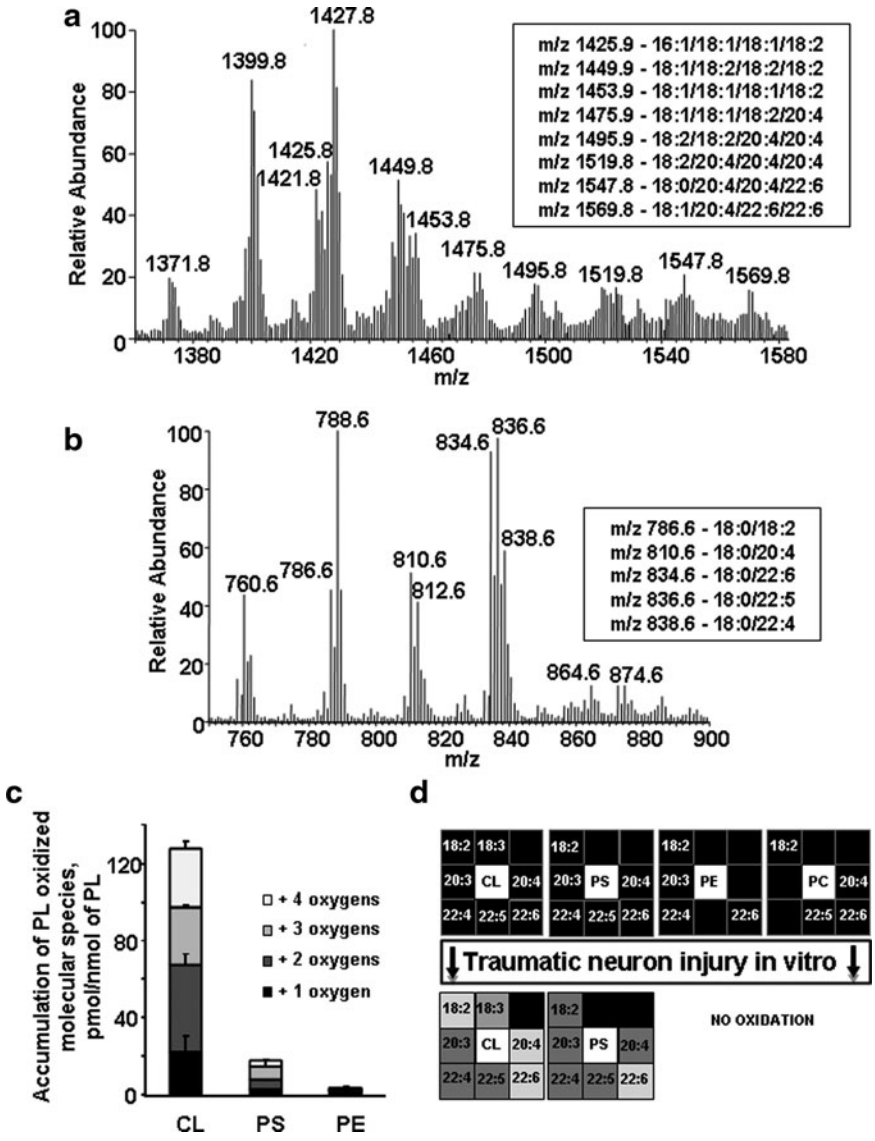

FIG. 6. Identification of phospholipid molecular species by liquid chromatography mass spectrometry (LC-MS). (**a**) Typical liquid chromatography electrospray ionization mass spectrometry (LC/ESI-MS) spectrum of CL isolated from control neurons. Insert: Major molecular species of CL containing polyunsaturated fatty acids. (**b**) Typical LC/ESI-MS spectrum of PS isolated from control neurons. Insert: Major molecular species of PS containing polyunsaturated fatty acids. (**c**) Accumulation of oxygenated phospholipids in rat cortical neurons 2 h after stretch assessed by LC-MS. Data are mean ± SD, $n = 3$. CL, cardiolipin; PS, phosphatidylserine; PE, phosphatidylethanolamine. (**d**) Oxidative lipidomics "Hit-map" of stretched neurons.

course of apoptotic events was different in stretched neurons (Stoica et al., 2003; Tyurin et al., 2008). In stretch-induced apoptosis, cyt c release into cytosol is unusually fast and there is a delay in caspase activation. The early release of cyt c can be caused by mechanical deformation of the outer mitochondrial membrane with stretch injury and subsequent release of cyt c. There could be several reasons for the observed delay in cyt c release and caspase activation. The initial appearance of small amounts of cyt c triggers a positive feedback loop and further release of cyt c from mitochondria, eventually causing caspase activation. In addition, we have shown that during apoptosis, released cyt c is scavenged by α-synuclein in the cytosol, preventing its interaction with apoptotic protease activating factor 1 (APAF-1) (Bayir et al., 2009). Nevertheless, significant amounts of cyt c remained confined within the mitochondrial compartments at early and late time points after the injury, possibly indicating its association with less damaged mitochondria in the soma of neurons.

Another mitochondrial event essential for the release of pro-apoptotic factors from mitochondria into the cytosol is robust oxidation of CL (Kagan et al., 2005; Tyurina et al., 2006). CL oxidation in neurons was detected as early as 2 h after stretch, when caspases were not activated yet mitochondria in neurites were damaged. Studies from several laboratories documented that execution of the mitochondrial stage of apoptosis is accompanied by oxidation of CL (Iverson and Orrenius, 2004; Kagan et al., 2005; Petrosillo et al., 2006). We discovered that CL represents a selective target of oxidative attack during apoptosis whereby cyt c forms

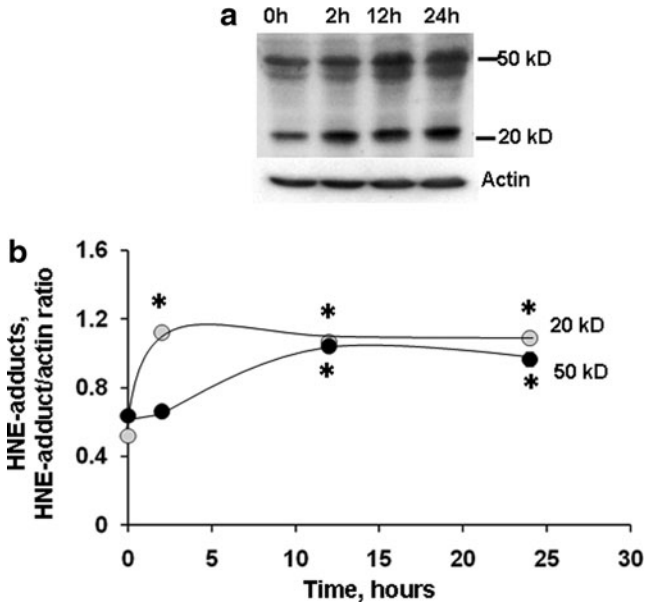

FIG. 7. Formation of HNE-protein adducts in P2 fraction isolated from primary neurons after stretch injury. Using Western blot **(a)**, anti-HNE antibody detected several protein bands with masses ranging from over 50 kD to less than 20 kD in cortical neurons cultured on elastic membranes. Increased levels of HNE protein adducts were observed after stretch **(b)**. Data are mean ± SD, $*p < 0.05$ vs. respective control, $n = 3$.

complexes with CL and catalyzes oxidation of the latter (Kagan et al., 2005; Tyurina et al., 2006). Most importantly, CL oxidation products are essential for the mitochondrial permeability transition and the release of pro-apoptotic factors into the cytosol (Kagan et al., 2005).

In the stretched neurons, we observed small but significant amount of Annexin V positivity as early as 30 min after injury. This may be caused, at least in part, by a transient permeabilization of plasma membrane at damaged sites of processes resulting in possible binding of Annexin V to PS in the inner leaflet of the plasma membrane. Acute plasmalemma damage and permeability has been well documented after TBI both *in vivo* and *in vitro* (Geddes et al., 2003; Geddes-Klein et al., 2006; Whalen et al., 2008). In line with earlier published data, caspase-3 activation is associated with nuclear shrinkage, fragmentation, and apoptotic body formation after mechanical stretch injury (Pike et al., 2000). We found that caspase-3 was significantly activated 12–24 h after stretch. Usually, during caspase-dependent intrinsic apoptosis, caspase activation is followed by PS oxidation and then PS externalization (Kagan et al., 2005). We have shown that cyt c plays an important role in PS oxidation and externalization (Jiang et al., 2004). It is possible that a fraction of the released cyt c interacts with PS resulting in the formation of cyt c/PS complex with peroxidase activity (Kapralov et al., 2007) that induces the accumulation of PS oxidation (PSox) products. PSox are important contributors to externalization of PS on the surface of apoptotic cells and their subsequent clearance (Kagan et al., 2003; Tyurina et al., 2004).

Several interrelated pathways of cell death – necrosis, necroptosis, caspase-dependent and caspase-independent apoptosis – can occur after stretch injury (Stoica and Faden, 2010). Improvement in cell survival by pre-treatment with a pan-caspase inhibitor, z-VAD-FMK (Pop et al., 2008), suggests that the caspase-dependent pathway is playing an important role in stretch-induced neuronal death in our model. However, as mentioned, Z-VAD-FMK did not completely attenuate the stretch-induced neuronal death, suggesting that other pathways of cell death are also operating after stretch injury. Interestingly, z-VAD-FMK also protected against accumulation of PI(+)/Annexin V(-) cells as well as against LDH release from injured neurons, therefore indicating that caspase-driven mechanisms also participated in the necrotic cell death pathway; that is, there was a crosstalk between these two cell death pathways. One may assume that incomplete apoptosis and subsequent necrosis are interconnected resulting in the sensitivity of the latter to z-VAD-FMK (Dietz et al., 2007; Suzuki and Koike, 2005). It is also possible that caspase-independent apoptotic mechanisms (e.g., calpain-mediated and apoptosis-inducing factor [AIF]-dependent pathways [Cao et al., 2007]) and necrosis also interact. Furthermore, it has been shown that z-VAD-FMK can also inhibit non-caspase proteases such as cathepsins (Chauvier et al., 2007). Cathepsins have been implicated in trauma-induced neuronal death. It has been shown that pre-treatment of mice with a cathepsin B inhibitor administered intracerebroventricularly decreases the number of PI (+) neurons in cortex after weight drop injury (Luo et al., 2010).

Prevention of CL oxidation may be a preferred target for anti-apoptotic strategies to protect neurons. Pre-treatment of neurons with *N*-acetylcysteine resulted in a significant but modest protective effect against stretch-induced cell death compared with z-VAD-FMK. It is possible that non-mitochondria-targeted *N*-acetylcysteine failed to increase mitochondrial glutathione levels high enough to combat ROS produced during neuronal apoptosis. Indeed, recent studies showed that *N*-acetylcysteine, at a concentration similar to the one used in our studies, did not have a significant effect on superoxide and hydrogen peroxide levels in mitochondria, whereas a mitochondria-targeted antioxidant SS-31 substantially reduced generation of superoxide and hydrogen peroxide in primary cardiomyocytes (Dai et al., 2007). Hydrogen peroxide feeds the catalytic peroxidase cycle leading to CL peroxidation. Therefore, in the absence of *N*-acetylcysteine-driven hydrogen peroxide consumption it is likely that CL peroxidation triggered by stretch remained unchanged. Corroborating this, mitochondria-targeted electron scavengers (nitroxides conjugated with hemigramicidin S or tri-phenylphosphonium), which prevent mitochondrial superoxide formation, have been shown to effectively safeguard cells against pro-apoptotic agents (Jiang et al., 2008) *in vitro,* and exert protective effects *in vivo,* after insults associated with significant accumulation of apoptotic cells (i.e., ionizing irradiation or hemorrhagic shock) (Jiang et al., 2008; Macias et al., 2007). Therefore, our data invoke reasonable optimism toward potentially useful applications of the mitochondria-targeted inhibitors of CL oxidation as anti-apoptotic neuroprotectors after brain trauma. Indeed, our preliminary experiments demonstrated the usefulness and effectiveness of a hemigramicidin S/nitroxide conjugate, XJB-5-131, to exert significant protection of young rats against TBI-induced damage, as evidenced by both biochemical and functional assessments (Ji et al., 2010). Corroborating the notion that mitochondrial lipid peroxides are effective therapeutic targets

after TBI, Mustafa and associates showed that U-83836E, a selective scavenger of lipid peroxyl radicals, reduced lipid peroxidation and improved bioenergetics in mitochondria after TBI (Mustafa et al., 2010).

Acknowledgments

This work was ssupported by grants from the National Institute of Health (HL70755, U19AI068021, NS061817) and by the Defense Advanced Research Projects Agency Preventing Violent Explosive Neurologic Trauma (DARPA PREVENT) blast program N66001-10-C-2124. The views, opinions, and/or findings contained in this article should not be interpreted as representing the official views or policies, either expressed or implied, of DARPA or the Department of Defense.

Author Disclosure Statement

No competing financial interests exist.

References

Ainslie, K.M., Tao, S.L., Popat, K.C., and Desai, T.A. (2008). In vitro immunogenicity of silicon-based micro- and nanostructured surfaces. ACS Nano 2, 1076–1084.

Arundine, M., Aarts, M., Lau, A., and Tymianski, M. (2004). Vulnerability of central neurons to secondary insults after in vitro mechanical stretch. J. Neurosci. 24, 8106–8123.

Barbee, K.A., Macarak, E.J., and Thibault, L.E. (1994). Strain measurements in cultured vascular smooth muscle cells subjected to mechanical deformation. Ann. Biomed. Eng. 22, 14–22.

Bayir, H., Kapralov, A.A., Jiang, J., Huang, Z., Tyurina, Y.Y., Tyurin, V.A., Zhao, Q., Belikova, N.A., Vlasova, II, Maeda, A., Zhu, J., Na, H.M., Mastroberardino, P.G., Sparvero, L.J., Amoscato, A.A., Chu, C.T., Greenamyre, J.T. and Kagan, V.E. (2009). Peroxidase mechanism of lipid-dependent cross-linking of synuclein with cytochrome C: protection against apoptosis versus delayed oxidative stress in Parkinson disease. J. Biol. Chem. 284, 15,951–15,969.

Bayir, H., Tyurin, V.A., Tyurina, Y.Y., Viner, R., Ritov, V., Amoscato, A.A., Zhao, Q., Zhang, X.J., Janesko–Feldman, K.L., Alexander, H., Basova, L.V., Clark, R.S., Kochanek, P.M., and Kagan, V.E. (2007). Selective early cardiolipin peroxidation after traumatic brain injury: an oxidative lipidomics analysis. Ann. Neurol. 62, 154–169.

Borisenko, G.G., Kapralov, A.A., Tyurin, V.A., Maeda, A., Stoyanovsky, D.A., and Kagan, V.E. (2008). Molecular design of new inhibitors of peroxidase activity of cytochrome c/cardiolipin complexes: fluorescent oxadiazole-derivatized cardiolipin. Biochemistry 47, 13,699–13,710.

Böttcher, C.S.F., Van Gent, C.M., and Fries, C. (1961). A rapid and sensitive sub-micro phosphorus determination. Anal. Chim. Acta 24, 203–204.

Brophy, G.M., Pineda, J.A., Papa, L., Lewis, S.B., Valadka, A.B., Hannay, H.J., Heaton, S.C., Demery, J.A., Liu, M.C., Tepas, J.J., 3rd, Gabrielli, A., Robicsek, S., Wang, K.K., Robertson, C.S., and Hayes, R.L. (2009). alphaII-Spectrin breakdown product cerebrospinal fluid exposure metrics suggest differences in cellular injury mechanisms after severe traumatic brain injury. J. Neurotrauma 26, 471–479.

Cao, G., Xing, J., Xiao, X., Liou, A.K., Gao, Y., Yin, X.M., Clark, R.S., Graham, S.H., and Chen, J. (2007). Critical role of calpain I in mitochondrial release of apoptosis-inducing factor in ischemic neuronal injury. J. Neurosci. 27, 9278–9293.

Cardaci, S., Filomeni, G., Rotilio, G., and Ciriolo, M.R. (2008). Reactive oxygen species mediate p53 activation and apoptosis induced by sodium nitroprusside in SH-SY5Y cells. Mol. Pharmacol. 74, 1234–1245.

Chauvier, D., Ankri, S., Charriaut–Marlangue, C., Casimir, R., and Jacotot, E. (2007). Broad-spectrum caspase inhibitors: from myth to reality? Cell Death Differ. 14, 387–391.

Clark, R.S., Bayir, H., Chu , C.T., Alber, S.M., Kochanek, P.M., and Watkins, S.C. (2008). Autophagy is increased in mice after traumatic brain injury and is detectable in human brain after trauma and critical illness. Autophagy 4, 88–90.

Dai, D.F., Chen, T., Szeto, H., Nieves–Cintron, M., Kutyavin, V., Santana, L.F., and Rabinovitch, P.S. (2011). Mitochondrial targeted antioxidant Peptide ameliorates hypertensive cardiomyopathy. J. Am. Coll. Cardiol. 58, 73–82.

Dietz, G.P., Dietz, B., and Bahr, M. (2007). Bcl-xL protects cerebellar granule neurons against the late phase, but not against the early phase of glutamate–induced cell death. Brain Res. 1164, 136–141.

Fadeel, B. (2003). Programmed cell clearance. Cell Mol. Life Sci. 60, 2575–2585.

Fiskum, G. (2000). Mitochondrial participation in ischemic and traumatic neural cell death. J. Neurotrauma 17, 843–855.

Folch, J., Lees, M., and Sloane Stanley, G.H. (1957). A simple method for the isolation and purification of total lipides from animal tissues. J. Biol. Chem. 226, 497–509.

Gartlon, J., Kinsner, A., Bal–Price, A., Coecke, S., and Clothier, R.H. (2006). Evaluation of a proposed in vitro test strategy using neuronal and non-neuronal cell systems for detecting neurotoxicity. Toxicol. In Vitro 20, 1569–1581.

Geddes, D.M., Cargill, R.S., 2nd, and LaPlaca, M.C. (2003). Mechanical stretch to neurons results in a strain rate and magnitude-dependent increase in plasma membrane permeability. J. Neurotrauma 20, 1039–1049.

Geddes–Klein, D.M., Schiffman, K.B., and Meaney, D.F. (2006). Mechanisms and consequences of neuronal stretch injury in vitro differ with the model of trauma. J. Neurotrauma 23, 193–204.

Gil-ad, I., Shtaif, B., Shiloh, R., and Weizman, A. (2001). Evaluation of the neurotoxic activity of typical and atypical neuroleptics: relevance to iatrogenic extrapyramidal symptoms. Cell Mol. Neurobiol. 21, 705–716.

Iverson, S.L., and Orrenius, S. (2004). The cardiolipin-cytochrome c interaction and the mitochondrial regulation of apoptosis. Arch. Biochem. Biophys. 423, 37–46.

Ji, J., Kline, A.E.P.J., Cheng, J.P., Wipf, P., Alexander, H., Kochanek, P.M., Kagan, V.E., and Bayir, H. (2010). Mitochondria-targeted nitroxide therapy prevents cytochrome c release and improves neurobehavioral outcome in pediatric traumatic brain injury. J. Neurotrauma 5, A-1–A-97.

Jiang, J., Belikova, N.A., Hoye, A.T., Zhao, Q., Epperly, M.W., Greenberger, J.S., Wipf, P., and Kagan, V.E. (2008). A mitochondria-targeted nitroxide/hemigramicidin S conjugate protects mouse embryonic cells against gamma irradiation. Int. J. Radiat. Oncol. Biol. Phys. 70, 816–825.

Jiang, J., Kini, V., Belikova, N., Serinkan, B.F., Borisenko, G.G., Tyurina, Y.Y., Tyurin, V.A., and Kagan, V.E. (2004). Cytochrome c release is required for phosphatidylserine peroxidation during Fas-triggered apoptosis in lung epithelial A549 cells. Lipids 39, 1133–1142.

Kagan, V.E., Bayir, A., Bayir, H., Stoyanovsky, D., Borisenko, G.G., Tyurina, Y.Y., Wipf, P., Atkinson, J., Greenberger, J.S.,

Chapkin, R.S., and Belikova, N.A. (2009). Mitochondria-targeted disruptors and inhibitors of cytochrome c/cardiolipin peroxidase complexes: a new strategy in anti-apoptotic drug discovery. Mol. Nutr. Food Res. 53, 104–114.

Kagan, V.E., Borisenko, G.G., Serinkan, B.F., Tyurina, Y.Y., Tyurin, V.A., Jiang, J., Liu, S.X., Shvedova, A.A., Fabisiak, J.P., Uthaisang, W., and Fadeel, B. (2003). Appetizing rancidity of apoptotic cells for macrophages: oxidation, externalization, and recognition of phosphatidylserine. Am. J. Physiol. Lung Cell Mol. Physiol. 285, L1–17.

Kagan, V.E., Tyurin, V.A., Jiang, J., Tyurina, Y.Y., Ritov, V.B., Amoscato, A.A., Osipov, A.N., Belikova, N.A., Kapralov, A.A., Kini, V., Vlasova, II, Zhao, Q., Zou, M., Di, P., Svistunenko, D.A., Kurnikov, I.V., and Borisenko, G.G. (2005). Cytochrome c acts as a cardiolipin oxygenase required for release of proapoptotic factors. Nat Chem Biol. 1, 223–232.

Kapralov, A.A., Kurnikov, I.V., Vlasova, II, Belikova, N.A., Tyurin, V.A., Basova, L.V., Zhao, Q., Tyurina, Y.Y., Jiang, J., Bayir, H., Vladimirov, Y.A., and Kagan, V.E. (2007) The hierarchy of structural transitions induced in cytochrome c by anionic phospholipids determines its peroxidase activation and selective peroxidation during apoptosis in cells. Biochemistry 46, 14,232–14,244.

Kiebish, M.A., Han, X., Cheng, H., Lunceford, A., Clarke, C.F., Moon, H., Chuang, J.H., and Seyfried, T.N. (2008). Lipidomic analysis and electron transport chain activities in C57BL/6J mouse brain mitochondria. J. Neurochem. 106, 299–312.

Kilinc, D., Gallo, G., and Barbee, K.A. (2008). Mechanically-induced membrane poration causes axonal beading and localized cytoskeletal damage. Exp. Neurol. 212, 422–430.

Kroemer, G., Galluzzi, L., and Brenner, C. (2007). Mitochondrial membrane permeabilization in cell death. Physiol. Rev. 87, 99–163.

Kuznetsov, A.V., Hermann, M., Saks, V., Hengster, P., and Margreiter, R. (2009). The cell-type specificity of mitochondrial dynamics. Int. J. Biochem. Cell Biol. 41, 1928–1939.

Lahiry, L., Saha, B., Chakraborty, J., Bhattacharyya, S., Chattopadhyay, S., Banerjee, S., Choudhuri, T., Mandal, D., Bhattacharyya, A., Sa, G., and Das, T. (2008). Contribution of p53-mediated Bax transactivation in theaflavin-induced mammary epithelial carcinoma cell apoptosis. Apoptosis 13, 771–781.

Lai, J.C., Walsh, J.M., Dennis, S.C., and Clark, J.B. (1977). Synaptic and non-synaptic mitochondria from rat brain: isolation and characterization. J. Neurochem. 28, 625–631.

LaPlaca, M.C., Lee, V.M., and Thibault, L.E. (1997). An in vitro model of traumatic neuronal injury: loading rate-dependent changes in acute cytosolic calcium and lactate dehydrogenase release. J. Neurotrauma 14, 355–368.

LaPlaca, M.C., and Thibault, L.E. (1997). An in vitro traumatic injury model to examine the response of neurons to a hydrodynamically-induced deformation. Ann. Biomed. Eng. 25, 665–677.

Lewen, A., Fujimura, M., Sugawara, T., Matz, P., Copin, J.C., and Chan, P.H. (2001). Oxidative stress-dependent release of mitochondrial cytochrome c after traumatic brain injury. J. Cereb. Blood Flow Metab. 21, 914–920.

Li, P.F., Dietz, R., and von Harsdorf, R. (1999). p53 regulates mitochondrial membrane potential through reactive oxygen species and induces cytochrome c-independent apoptosis blocked by Bcl-2. EMBO J. 18, 6027–6036.

Liu, C.L., Chen, S., Dietrich, D., and Hu, B.R. (2008). Changes in autophagy after traumatic brain injury. J. Cereb. Blood Flow Metab. 28, 674–683.

Luo, C.L., Chen, X.P., Yang, R., Sun, Y.X., Li, Q.Q., Bao, H.J., Cao, Q.Q., Ni, H., Qin, Z.H., and Tao, L.Y. (2010). Cathepsin B contributes to traumatic brain injury-induced cell death through a mitochondria-mediated apoptotic pathway. J. Neurosci. Res. 88, 2847–2858.

Lusardi, T.A., Rangan, J., Sun, D., Smith, D.H., and Meaney, D.F. (2004). A device to study the initiation and propagation of calcium transients in cultured neurons after mechanical stretch. Ann. Biomed. Eng. 32, 1546–1558.

Macias, C.A., Chiao, J.W., Xiao, J., Arora, D.S., Tyurina, Y.Y., Delude, R.L., Wipf, P., Kagan, V.E., and Fink, M.P. (2007). Treatment with a novel hemigramicidin-TEMPO conjugate prolongs survival in a rat model of lethal hemorrhagic shock. Ann. Surg. 245, 305–314.

Mironov, S.L. (2009). Complexity of mitochondrial dynamics in neurons and its control by ADP produced during synaptic activity. Int. J. Biochem. Cell Biol. 41, 2005–2014.

Murphy, E.J., and Horrocks, L.A. (1993). A model for compression trauma: pressure-induced injury in cell cultures. J. Neurotrauma 10, 431–444.

Mustafa, A.G., Singh, I.N., Wang, J., Carrico, K.M., and Hall, E.D. (2010). Mitochondrial protection after traumatic brain injury by scavenging lipid peroxyl radicals. J. Neurochem. 114, 271–280.

Okonkwo, D.O., and Povlishock, J.T. (1999). An intrathecal bolus of cyclosporin A before injury preserves mitochondrial integrity and attenuates axonal disruption in traumatic brain injury. J. Cereb. Blood Flow Metab. 19, 443–451.

Pedersen, M.O., Larsen, A., Stoltenberg, M., and Penkowa, M. (2009). Cell death in the injured brain: roles of metallothioneins. Prog. Histochem. Cytochem. 44, 1–27.

Petrosillo, G., Casanova, G., Matera, M., Ruggiero, F.M., and Paradies, G. (2006). Interaction of peroxidized cardiolipin with rat-heart mitochondrial membranes: induction of permeability transition and cytochrome c release. FEBS Lett. 580, 6311–6316.

Pike, B.R., Zhao, X., Newcomb, J.K., Glenn, C.C., Anderson, D.K., and Hayes, R.L. (2000). Stretch injury causes calpain and caspase-3 activation and necrotic and apoptotic cell death in septo-hippocampal cell cultures. J. Neurotrauma 17, 283–298.

Polster, B.M., and Fiskum, G. (2004). Mitochondrial mechanisms of neural cell apoptosis. J. Neurochem. 90, 1281–1289.

Pop, C., Salvesen, G.S., and Scott, F.L. (2008). Caspase assays: identifying caspase activity and substrates in vitro and in vivo. Methods Enzymol. 446, 351–367.

Robertson, C.L. (2004). Mitochondrial dysfunction contributes to cell death following traumatic brain injury in adult and immature animals. J. Bioenerg. Biomembr. 36, 363–368.

Rouser, G., Fkeischer, S., and Yamamoto, A. (1970). Two dimensional then layer chromatographic separation of polar lipids and determination of phospholipids by phosphorus analysis of spots. Lipids 5, 494–496.

Samali, A., Zhivotovsky, B., Jones, D., Nagata, S., and Orrenius, S. (1999). Apoptosis: cell death defined by caspase activation. Cell Death Differ. 6, 495–496.

Schlame, M. (2008). Cardiolipin synthesis for the assembly of bacterial and mitochondrial membranes. J. Lipid Res. 49, 1607–1620.

Schwartz, J.C., Syka, J.E.P., and Quarmby, S.T. (2005). Improving the fundamentals of MSn on 2D linear uon traps: new ion activation and isolation techniques, in: Proceedings of the 53rd American Society for Mass Spectrometry and Allied Topics, San Antonio, Texas.

Shimazawa, M., and Hara, H. (2006). Inhibitor of double stranded RNA-dependent protein kinase protects against cell damage induced by ER stress. Neurosci. Lett. 409, 192–195.

Shimazawa, M., Ito, Y., Inokuchi, Y., and Hara, H. (2007). Involvement of double-stranded RNA-dependent protein kinase in ER stress-induced retinal neuron damage. Invest. Ophthalmol. Vis. Sci. 48, 3729–3736.

Singh, I.N., Sullivan, P.G., Deng, Y., Mbye, L.H., and Hall, E.D. (2006). Time course of post-traumatic mitochondrial oxidative damage and dysfunction in a mouse model of focal traumatic brain injury: implications for neuroprotective therapy. J. Cereb. Blood Flow. Metab. 26, 1407–1418.

Slemmer, J.E., Zhu, C., Landshamer, S., Trabold, R., Grohm, J., Ardeshiri, A., Wagner, E., Sweeney, M.I., Blomgren, K., Culmsee, C., Weber, J.T., and Plesnila, N. (2008). Causal role of apoptosis-inducing factor for neuronal cell death following traumatic brain injury. Am. J. Pathol. 173, 1795–1805.

Sparvero, L.J., Amoscato, A.A., Kochanek, P.M., Pitt, B.R., Kagan, V.E., and Bayir, H. (2010). Mass-spectrometry based oxidative lipidomics and lipid imaging: applications in traumatic brain injury. J. Neurochem. 115, 1322–1336.

Stoica, B.A., and Faden, A.I. (2010). Cell death mechanisms and modulation in traumatic brain injury. Neurotherapeutics 7, 3–12.

Stoica, B.A., Movsesyan, V.A., Lea, P.M.T., and Faden, A.I. (2003). Ceramide-induced neuronal apoptosis is associated with dephosphorylation of Akt, BAD, FKHR, GSK-3beta, and induction of the mitochondrial-dependent intrinsic caspase pathway. Mol. Cell Neurosci. 22, 365–382.

Sullivan, P.G., Bruce–Keller, A.J., Rabchevsky, A.G., Christakos, S., Clair, D.K., Mattson, M.P., and Scheff, S.W. (1999). Exacerbation of damage and altered NF-kappaB activation in mice lacking tumor necrosis factor receptors after traumatic brain injury. J Neurosci. 19, 6248–6256.

Suzuki, M., and Koike, T. (2005). Early apoptotic and late necrotic components associated with altered Ca2+ homeostasis in a peptide-delivery model of polyglutamine-induced neuronal death. J. Neurosci. Res. 80, 549–561.

Tyurin, V.A., Tyurina, Y.Y., Feng, W., Mnuskin, A., Jiang, J., Tang, M., Zhang, X., Zhao, Q., Kochanek, P.M., Clark, R.S., Bayir, H., and Kagan, V.E. (2008). Mass-spectrometric characterization of phospholipids and their primary peroxidation products in rat cortical neurons during staurosporine-induced apoptosis. J. Neurochem. 107, 1614–1633.

Tyurina, Y.Y., Kini, V., Tyurin, V.A., Vlasova, II, Jiang, J., Kapralov, A.A., Belikova, N.A., Yalowich, J.C., Kurnikov, I.V., and Kagan, V.E. (2006). Mechanisms of cardiolipin oxidation by cytochrome c: relevance to pro- and antiapoptotic functions of etoposide. Mol. Pharmacol. 70, 706–717.

Tyurina, Y.Y., Tyurin, V.A., Zhao, Q., Djukic, M., Quinn, P.J., Pitt, B.R., and Kagan, V.E. (2004). Oxidation of phosphatidylserine: a mechanism for plasma membrane phospholipid scrambling during apoptosis? Biochem. Biophys. Res. Commun. 324, 1059–1064.

Verweij, B.H., Muizelaar, J.P., Vinas, F.C., Peterson, P.L., Xiong, Y., and Lee, C.P. (1997). Mitochondrial dysfunction after experimental and human brain injury and its possible reversal with a selective N-type calcium channel antagonist (SNX–111). Neurol. Res. 19, 334–339.

Whalen, M.J., Dalkara, T., You, Z., Qiu, J., Bermpohl, D., Mehta, N., Suter, B., Bhide, P.G., Lo, E.H., Ericsson, M., and Moskowitz, M.A. (2008). Acute plasmalemma permeability and protracted clearance of injured cells after controlled cortical impact in mice. J. Cereb. Blood Flow Metab. 28, 490–505.

Xiong, Y., Gu, Q., Peterson, P.L., Muizelaar, J.P., and Lee, C.P. (1997). Mitochondrial dysfunction and calcium perturbation induced by traumatic brain injury. J. Neurotrauma 14, 23–34.

Yang, L., Zhang, B., Toku, K., Maeda, N., Sakanaka, M., and Tanaka, J., 2000. Improvement of the viability of cultured rat neurons by the non-essential amino acids L-serine and glycine that upregulates expression of the anti-apoptotic gene product Bcl-w. Neurosci. Lett. 295, 97–100.

Zhivotovsky, B., Samali, A., Gahm, A., and Orrenius, S. (1999). Caspases: their intracellular localization and translocation during apoptosis. Cell Death Differ. 6, 644–651.

Zielonka, J., and Kalyanaraman, B. (2010). Hydroethidine- and MitoSOX-derived red fluorescence is not a reliable indicator of intracellular superoxide formation: another inconvenient truth. Free Radic. Biol. Med. 48, 983–1001.

Address correspondence to:
Yulia Y. Tyurina, Ph.D.
Bridgeside Point
100 Technology Drive, Suite 350
Pittsburgh, PA, 15219

E-mail: yyt1@pitt.edu

or

Hülya Bayır, M.D.
3434 Fifth Avenue
Pittsburgh, PA 15213

E-mail: bayihx@ccm.upmc.edu